Published in final edited form as:
Sci Total Environ. 2018 February 01; 613-614: 714–723. doi:10.1016/j.scitotenv.2017.09.050.

Dermal Transfer and Environmental Release of CeO_2 Nanoparticles Used as UV Inhibitors on Outdoor Surfaces: Implications for Human and Environmental Health

Justin G. Clar[‡,†], **William E. Platten III**[¥], **Eric J. Baumann Jr**[¥], **Andrew Remsen**[¥], **Steve M. Harmon**[‡], **Christina L. Bennett-Stamper**[‡], **Treye A. Thomas**[§], **Todd P. Luxton**[‡,*]

[‡]National Risk Management Research Laboratory, Office of Research and Development, U.S., Environmental Protection Agency, 5995 Center Hill Avenue, Cincinnati, OH 45224, USA

[¥]Pegasus Technical Services Inc, Cincinnati OH

[†]Oak Ridge Institute for Science and Education (ORISE) Postdoctoral Research Associate

[§]U.S. Consumer Product Safety Commission, Office of Hazard Identification and Reduction, 4330 East West Highway, Bethesda, MD 20814

Abstract

A major area of growth for “nano-enabled” consumer products have been surface coatings, including paints stains and sealants. Ceria (CeO_2) nanoparticles (NPs) are of interest as they have been used as additive these products to increase UV resistance. Currently, there is a lack of detailed information on the potential release and, and speciation (*i.e.*, ion vs. particle) of CeO_2 NPs used in consumer-available surface coatings during intended use scenarios. In this study, both Micronized-Copper Azole pressure-treated lumber (MCA), and a commercially available composite decking were coated with CeO_2 NPs dispersed in Milli-Q Water or wood stain. Coated surfaces were divided into two groups. The first was placed outdoors to undergo environmental weathering, while the second was placed indoors to act as experimental controls. Both weathered surfaces and controls were sampled over a period of 6 months via simulated dermal contact using methods developed by the Consumer Product Safety Commission (CPSC). The size and speciation of released material was determined through sequential filtration, total metals analysis, X-Ray Absorption Fine Structure Spectroscopy, and electron microscopy. The total ceria release from MCA coated surfaces was found to be dependent on dispersion matrix with aqueous applications releasing greater quantities more than stain based applications, 66 ± 12 mg/m^2 and 36 ± 7 mg/m^2, respectively. Additionally, a substantial reduction of CeO_2 to Ce(III)-organic complexes is observed over the 6-month experimental period in aqueous based applications.

* Luxton.Todd@epa.gov, (513) 569-7210.
Current Addresses
J.G.C – Department of Chemistry, Elon University, 2625 Campus Box, Elon NC 27244
W.E.P – U.S. EPA, Office of Water, Cincinnati OH

Supporting Information
Additional text, one table, and 11 figures showing additional details of nanoparticle characterization, XPS analysis, SEM images, model XAFS spectra and examples of LCF analysis. This material is available free of charge via the Internet at: http://pubs.acs.org.

Introduction

Research and development of Engineered Nanomaterials (ENMs) has continued to expand over the last two decades, resulting in nano-enabled products available in both industrial and commercial settings. One area of particular growth for ENMs has been surface coatings, including paints, stains, lacquers and sealants(Kaiser et al., 2013b; Lee et al., 2010; van Broekhuizen et al., 2011). ENMs have been added to these products for a variety of desired outcomes, including antimicrobial activity (Kaiser et al., 2013a), increased scratch resistance (Hwang et al., 2003; Zhou et al., 2002), hydrophobicity (Manoudis et al., 2009), and UV protection (Sawitowski, 2006). Unlike composite materials, where the ENMs are imbedded in a matrix, ENMs applied as surface coatings are readily available for interaction with the surrounding environment, and therefore increasing their potential for transformation, degradation, and release. Accordingly, material flow analysis conducted by Keller and coworkers has estimated that the vast majority of ENMs that will be released to both water and soil environments will originate from surface coating products (Keller et al., 2013).

While ceria nanoparticles (CeO_2 NPs) have been widely studied as diesel fuel catalysts and in electronic devices, there is a growing interest in their use as additives to surface coatings to increase UV protection and increase the longevity and improve the appearance of UV-exposed products, *e.g.*, outdoor wood surfaces and vinyl/aluminum siding (Auffan et al., 2014; Castano et al., 2015; Collin et al., 2014). The potential for widespread use of CeO_2 NPs as a UV protective agent stems from two important chemical properties. Unlike other metal oxide ENMs used in UV protection (*i.e.*, TiO_2), CeO_2 NPs do not undergo the same level of photocatalytic behavior resulting in unwanted free radical production (Faure et al., 2013). Additionally, CeO_2 NPs are thought to be highly stable and not prone to dissolution in a variety of environments (Dahle and Arai, 2015; Dahle et al., 2015). Although previously published research has attempted to track the release of ENM from surface coatings, these studies have focused on Ag, SiO_2, and TiO_2 (Al-Kattan et al., 2015; Al-Kattan et al., 2013; Kaegi et al., 2010; Kaegi et al., 2008; Shandilya et al., 2015; Zuin et al., 2013). However, recent research has estimated that between 5 percent to 10 percent of all industrially produced CeO_2 NPs are used in UV protective coatings and paints (Piccinno et al., 2012). Furthermore, these previous studies have focused solely on ENM release from surface coatings under passive release conditions (*i.e.*, leaching, runoff). Most studies have overlooked the release of the same material during physical contact, which may be the largest human exposure pathway to sensitive receptors, such as children, depending on where the product is applied.

The absence of published studies evaluating the release of ENMs from surface coatings through physical contact might be caused by the lack of validated methods to test potential exposure for specifically nano-enabled products. Simulated dermal transfer methods developed by the U.S. Consumer Product Safety Commission (CPSC) have been used in the past to estimate the release and transfer of arsenic from copper chromated arsenate lumber (Cobb, 2003; Thomas et al., 2005). More recently, this same method was adapted and successfully used by Platten and coworkers to estimate the release of copper particles from micronized copper pressure-treated lumber (Platten III et al., 2016). These early results suggest that the CPSC wipe methodology may be a strong candidate to evaluate ENM

release from surface coatings during dermal contact. Critically, modifications to the method allowed for determination of not only the total amounts of material dislodged from the surface, but also distinguish differences between ionic and particulate fractions. This differentiation is especially important for ENM toxicity because previous studies have suggested variations in biological response, based on size, morphology, and the presence of a capping agent. Understanding the form and species of material released from EMN surface coatings is particularly important in the case of cerium, due to the current controversy regarding its antioxidant properties (Lee et al., 2013) versus its ability to generate reactive oxygen species (ROS) (Zhang et al., 2011). Furthermore, understanding the release mechanisms and speciation aids in estimating the potential for exposure to sensitive populations.

In this study, commercially available CeO_2 NPs, marketed as an additive for increased UV protection for coated surfaces, were applied to both, micronized copper-azole pressure treated lumber (MCA) and a composite decking material. Estimates of dermal transfer from coated surfaces were evaluated using a wipe method developed by the CPSC (Cobb, 2003; Thomas et al., 2005) and previously applied to other nano-enabled materials (Platten III et al., 2016). Additionally, cerium release was also tracked during simulated leaching experiments. The goal of this work is twofold. Using the CPSC wipe method as a screening tool for ENM release from surface coatings, we track CeO_2 NP release during reasonably intended use scenarios. Moreover, we aim to understand both the nature and speciation of cerium released throughout the study to help inform environmental and human health risk assessments of these particles in consumer products and applications.

Materials and Methods

Surface Specimens:

Two commercially available products were selected for cerium application: micronized copper azole-treated lumber (MCA), and a widely available composite decking. These products were selected to provide a representative sample of surfaces on which UV protective paints, stains, and sealants may be applied. Both materials were purchased from national hardware retailers within a 50-mile radius of Cincinnati, OH. MCA and composite decking were purchased in bulk to minimize potential heterogeneity between production runs. MCA is produced from Southern Yellow Pine, while the composite decking is described as a combination of recycled plastics and refined wood fibers enclosed in a protective hydrophobic polymer cap. MCA samples were purchased in nominal dimensions of 5.08 cm × 15.24 cm × 2.43 m, while the composite decking purchased measured 2.36 cm × 13.26 cm × 4.9 m. Detailed characterization of the MCA-treated lumber can be found in our previous publication (Platten III et al., 2016).

Nanoparticle Characterization:

Ceria NPs were obtained from BYK (Germany) as liquid dispersions containing 10 nm particles stabilized with an ammonium citrate cap. These specific NPs were selected for use because they are advertised as an additive for water-based coatings that will increase resistance to UV degradation. Total metal analysis was completed through established

protocols (EPA Methods 3015A and 3051A) and analyzed for 28 separate metals by inductively coupled plasma-optical emission spectrometry to confirm cerium content, as well as identify impurities (ICP-OES, Thermo Fisher iCAP 6000 Series). After dilution in Milli-Q water (18.2 mΩ), all CeO_2 solutions were characterized for hydrodynamic diameter (HDD) using a ZetaSizer Nano Series (Malvern, Worcestershire, UK). HDD measurements were completed using an average of three runs, with each run consisting of at least 12 measurements. Additionally, primary particle size and morphology were determined using both Scanning Transmission Electron Microscopy (STEM), using a JEOL JEM-2100F (Peabody, MA), and Field Emission Scanning Electron Microscopy (FESEM), using a JEOL JSM-7600F (Tokyo, Japan). The relative abundance of Ce(III) and Ce(IV) present in the samples was determined by X-Ray Photoelectron spectroscopy (XPS), using a PHI Quantera II (Physical Electronics, Chanhassen, MN) and X-Ray Absorbance Fine Structure (XAFS) Spectroscopy. Details of STEM, FESEM, and XPS sample preparation are presented in the Supporting Information.

Coating Procedure and Experimental Design:

As directed by the manufacturer, CeO_2 stock solutions were diluted to 6 wt % before application to selected surfaces. To investigate the effect of application matrix on behavior, CeO_2 NPs were diluted in either Milli-Q Water or a commercially available water-based wood stain. (DEFY Stain for Hardwoods, Light Walnut) Initial analysis of the stain determined background cerium concentrations to be below the method detection limit. (0.230 mg/L) To ensure homogenization, all solutions were mixed for 20 min using a reciprocating shaker. Test solutions were applied to both MCA wood and composite decking by hand, using a 2-inch paint roller. Estimated volumes of applied solution were obtained by taking the difference of the mass of the paint tray and roller before and after application. Solutions were applied in two coats allowing at least 10 min for the initial coat to dry before application of the second coat. CeO_2 dispersed in wood stain was not applied to composite decking because it is not a realistic application of the product because the products are purchased in a variety of colors. After application of the second coat, all surfaces were allowed to air dry for at least 48 h before further use. The resulting samples were used for the simulated dermal contact experiments described below. An estimate of the average concentration of CeO_2 applied to the wood surfaces was determined by digesting a coupon of wood removed from a subset of the aqueous and stain suspensions after the 48-h curing process. Briefly, four 2.5 × 2.5 cm coupons, at least 0.5 mm in depth, were removed from the surface of the treated wood boards. The coupons were completely digested following EPA Method 3050B and subsequently analyzed by ICP-OES.

In addition to pristine surfaces coated with CeO_2 dispersions, a set of MCA boards were artificially weathered/aged inside a UV light chamber (UVA 340 nm) for 1260 h before coating. These samples are representative of aged wood surfaces that may undergo surface coatings by a consumer to extend their useful lifetime and prevent further degradation. These boards were aged in a continuous cycle of 3 h UV light exposure and 1 h “dark period” for system cool down until reaching a total of 1260 h of UV exposure. Once daily, the boards were removed from the unit and coated with Milli-Q water to add moisture to the system. During UV exposure, light intensity was kept at a constant irradiance of 0.5 $W/m^2/nm$. After

UV exposure, these MCA boards were coated identically to those previously described and placed back in the chamber to undergo additional UV exposure. Throughout additional exposure, boards were again coated once per day with Milli-Q water to add moisture to the system. The resulting samples were also used in simulated dermal contact experiments, described below.

Wiping Procedure:

For each experimental condition, (Water/Wood, Stain/Wood, Water/Composite) five 2 ft subsections were placed outside at the U.S. Environmental Protection Agency (EPA) Center Hill research facility in Cincinnati, OH, to investigate the effects of weathering (UV exposure, temperature variation, precipitation) on cerium release and transformation. Details of weather conditions can be found in the Supporting Information (Table S1, Figure S1). Additionally, four coated subsections were placed indoors, eliminating environmental variability. These indoor samples function as the experimental controls for the study. Both indoor and outdoor subsections were sampled periodically for 6 months, using a modified CPSC wipe method to estimate the release of the coatings during contact (Cobb, 2003; Platten III et al., 2016; Thomas et al., 2005). Finally, wipe results from the artificially degraded boards highlight potential changes in release patterns if a surface is aged prior to coating. These pre-weathers boards were placed back in the UV light chamber after coating and were sampled weekly for 8 weeks. For each condition (Outdoor, Indoor, Pre-Weathered), a minimum of four replicated where used in generating cerium release data. Differences in total cerium release between experimental treatments (Outdoor, Pre-Weathered) and controls (Indoor) were determined by a Fisher Least Significant Difference (LSD) Test. ($n= 4$; $\alpha = 0.05$).

Briefly, 10 cm square polyester fabric cloths were soaked in 2 mL of a NaCl solution for 24 hours before use. After soaking, cloths were attached to the head of the CPSC wiping apparatus, an 8-cm diameter aluminum disc with a mass of 1.1 kg (See Figures S2 and S3). The head of the apparatus (cloth attached) was dragged over a distance of 50 cm for an effective surface area of 450 cm^2. A wipe cycle consisted of moving the weight back and forth one time. Each sampling event consisted of 10 wipe cycles. After the first five wipe cycles, the disc and cloth were rotated 90 degrees before completing the remaining five wipe cycles. Post sampling, cloths were placed in separate 50 mL HDPE tubes and soaked in 20 mL of 10 % Nitric Acid and 20 % hydrogen peroxide and placed in a water bath at 60 ^0C for 24 h to solubilize metals of interest. Based upon preliminary investigations, the extraction solution was sufficiently caustic to completely dissolve CeO_2 over a 24 h period. Additionally, all samples were digested in parallel with reference materials to ensure quality control and recovery efficiency After cooling, samples were diluted with Milli-Q Water, when necessary, and analyzed by ICP-OES.

To determine the size and form of particulate matter dislodged from the boards during wiping, a single cloth was extracted, using a modified procedure. These cloths were placed in 20 mL of Milli-Q water and allowed to mix on a rotary shaker for at least 20 min. The resulting solution was sequential filtered through a 0.45 μm Track-Etched Membrane filter (Whatman), followed by a 10 kDa (~3–5 nm) Amicon Ultrafiltration filter (Millipore,

Billerica MA) and centrifuged at 4,500 g for 20 min, using a fixed-angle rotor. An unfiltered subsample, as well as 0.45 μm and 10 kDa filtrates, were acidified and processed by ICP-OES, while the solid filters were reserved for both SEM and metal speciation analysis. Images of the sampling apparatus and used polyester fabric cloths are presented in the Supporting Information (Figure S2–S3).

Leaching Procedure:

Samples used for leaching experiments were prepaid identically to those used in wipe studies. After drying, coated surfaces were cut into 4 cm × 4 cm coupons in preparation for leaching tests. Coupons were placed in separate 250 mL beakers, coated side down, which had been filled with 100 mL of Milli-Q water adjusted to pH 4.2 with synthetic precipitation leaching procedure (SPLP) solution. MCA samples easily floated in leaching solution, while composite decking samples were suspended with I-hooks to prevent them from sinking to the bottom of the container. All samples and controls (uncoated MCA and composite decking) were completed in quadruplicate and placed on a multi-positional magnetic stir-plate. Samples were covered and mixed at 200 RPM continuously for 72 h. At the end of mixing, a 20-mL aliquot was removed to determine total cerium concentration in the leachate. The remaining solution was then sequential filtered through 0.45 μm and 10 kDa (~3–5 nm) membranes to determine particle size fractionation. An unfiltered subsample, as well as 0.45 μm and 10 kDa filtrates were acidified and processed by ICP-OES, while the solid filters were reserved for both SEM and metal speciation analysis. All liquid solutions and the remaining 0.45 μm and 10 kDa filters were digested using established protocols (EPA Methods 3015A and 3051A) and analyzed for metal concentrations by inductively coupled plasma-optical emission spectrometry (ICP-OES, Thermo Fisher iCAP 6000 Series).

Metal Speciation by X-Ray Absorption Fine Structure Spectroscopy (XAFS):

To understand changes to speciation throughout weathering and leaching tests, XAFS spectra was collected on the initial CeO_2 NPs, as well as filters and wood blocks produced, by the wiping and leaching experiments. XAFS analyses were conducted at Sector 10BM (MRCAT) (Kropf et al., 2010) at the Advanced Photon Source at Argonne National Laboratory, U.S. Department of Energy, Argonne, IL. The incident beam was monochromatized by using a Si (111) fixed-exit, double-crystal monochromator. The beam size was focused to an area of 3000×500 μm. At least three scans were collected for each sample to optimize signal/noise ratio and collected in transmission and fluorescence mode simultaneously. Ce speciation was collected at the Ce-L3 edge (5723 eV) after calibration using a Cr foil (Cr-K edge 5989 eV). Solid standards used for data analysis were diluted with polyvinyl pyrrolidine (PVP), when necessary, and pressed in 13 mm diameter self-supported pellets and sealed in Kapton® tape before analysis. Liquid samples and standards were immobilized on sterile cotton swabs and also sealed in Kapton® polyimide tape. XAFS data reduction, including averaging, background removal by spline fitting, normalization and derivatization followed standard methods using the IFEFFIT software package (Ravel and Newville, 2005). Linear combination fitting (LCF) was conducted on normalized and first derivative spectra of the samples using the IFEFFIT computer software package to quantify metal speciation. The fitting range was −20 to 60 eV relative to the Ce-L3 edge.

Results and Discussion

Nanoparticle Characterization:

The NPs used throughout this study are listed by the manufacturer as 10 nm CeO_2 particles stabilized with an ammonium citrate cap to prevent particle aggregation. A detailed characterization of these particles is summarized in Table 1. While the HDD measurements are slightly smaller than those reported by the manufacturer, the distribution is very tight, centering around 8 nm. SEM/TEM images in Figure 1 show the spherical to hexagonal morphology of the CeO_2 particles with an observed diameter of 6.4±1.3 nm (average of 52 particles). XPS analysis indicates between 56 and 64% of the Ce in the sample is present as Ce(III) and not as Ce(IV). This range of speciation is slightly higher than previously reported CeO_2 NPs in the same size range (Deshpande et al., 2005) and might be a result of the citrate capping agent used to stabilize the particles, as well as the rigid level of restriction used in peak deconvolution. A detailed analysis of XPS fitting parameters can be found in the Supporting Information (Figures S4 and S5). Alternatively, XAFS analysis of the pristine material does not include a substantial amount of Ce(III) and matches nicely with an independent CeO_2 standard (not shown). The discrepancy between these two results can be explained by the nature of the analysis. The XAFS spectra obtained on this material is a bulk analysis, while XPS is a surface sensitive technique, only probing the first few angstroms of the particle surface (Hochella, 1988). Therefore, the relative percentage of Ce(III) reported in the XPS analysis is not unexpected as the indecent X-rays will over-sample the exterior Ce(III)-citrate bounds relative to the CeO_2 present in the bulk. While both the XPS and XAFS analysis demonstrate the presence of Ce(III) in the initial material, it is a minor component of the bulk phase.

Estimates of Dermal Transfer Using CPSC Methods:

Results of the cerium extraction from the cloths used during dermal transfer studies are presented in Figure 2. The cerium release for all experimental combinations has been normalized by the surface area wiped. Figure S6 in the Supporting Information presents the raw data in terms of total cerium release. Several interesting trends are observed in Figure 2. Immediately apparent are the large error bars seen in several of the experimental treatments. These large errors are explained by the heterogeneity of the wood and composite surfaces. The irregular nature of the surface can result in an abundance of cerium readily available for extraction in some areas of the board, while simultaneously trapping more cerium in cracks and crevasses in other sections. In general, the greatest release of cerium for all treatments is during the first sampling event. This is a logical result as the freshly applied coatings would be readily available at the surface for dermal contact and extraction. During continued wiping, the amount of cerium released decays to a steady state between two and five sampling events, depending on the experimental treatment.

The dispersion medium plays a significant role in the release of cerium during wiping events. When dispersed in water, cerium is readily removed from the surface during simulated dermal contact releasing between 17–27 mg/m^2 during the initial sampling event (10 passes sampling 450 cm^2). In contrast, when dispersed in the wood stain, cerium release decreases by roughly 50 percent, to 9–11 mg/m^2. In fact, throughout the duration of the

study, cerium dispersed in wood stain resulted in the lowest release of all test treatments. This consistency may be caused by the polymers and binders present in the wood stain that work to adhere the coating to the wood surface, limiting the release of CeO_2 NPs during simulated dermal contact.

While Ce release clearly diminishes to a steady state with increased contact events, determining the specific impact of the dispersion medium and weathering conditions is difficult. For example, during a single wipe event for a given treatment, samples aged outdoors may have resulted in higher Ce release compared to their indoor counterparts. However, the opposite trend would be observed at the next wipe event. Therefore, to investigate more directly the influence of dispersion media and weathering conditions on Ce release, the total amount of Ce released from all the wiping events during the 6-month period was calculated and the mean amount of Ce released for each treatment was compared using a Fisher LSD test ($\alpha = 0.05$) shown in Figure 3. A means comparison indicates that there was no statistical difference in the total Ce released between the indoor controls and outdoor treatment for the aqueous media application on lumber. This suggests that outdoor weathering may not have a significant effect on the extent of cerium release during dermal contact. Cerium release from stain based application resulted in significantly lower release. Interestingly, significant differences were observed between indoor controls and samples allowed to weather outdoors for the stain based application. The increased release of Ce from the outdoor stain/wood application compared to the indoor controls is attributed to deterioration of the stain due to environmental conditions, as evidenced by visual comparison of the indoor and outdoor treatments.

A similar analysis of the water/composite treatments highlights a significant decrease in the amount of Ce released from samples placed outdoors compared to indoor controls. Based on the hydrophobic polymer cap of the composite material itself, we hypothesize that the reduced amount of Ce recovered from the outdoor treatment is due to leaching from the surface during precipitation events, between the first and second sampling events, based on differences in the amount of Ce released (Figure 1). While the current data suggest that outdoor weathering has an impact on the amount of cerium released, the extent to which it functions as the dominant variable needs further investigation.

To estimate the relative percentage of cerium removed from the boards during dermal contact throughout the 6 months' study wood coupons (4) from unwiped sections of indoor control samples were removed and analyzed for cerium content. This analysis indicated roughly 110 mg of cerium were applied to each 2 ft sample section. Based on the total amount of cerium wiped from the surface of the indoor treatments, approximately 2.5 and 0.75% of the total applied cerium was wiped from the surface of the aqueous and stain treatments, respectively. The small quantity of material released would indicate that the majority of CeO_2 applied is not readily dislodged from the wood surface.

Estimates of Dermal Transfer from Pre-Weathered Boards:

To determine how the nature of the initial surface (*i.e.*, fresh vs. aged) affects the cerium release from the surface coatings, a portion of MCA boards were artificially aged using a UV light chamber, as described in the Material and Methods section. After coating, these

degraded boards were returned to the UV light chamber for further exposure and sampled weekly. This experimental setup allows for continued UV exposure without adding environmental factors, such as temperature fluctuation and precipitation. Normalized cerium release data are presented in Figure 4. Figure S7 in the Supporting Information section presents the raw data in terms of total cerium release. In this controlled system, the effect of the dispersion medium is again apparent, with cerium release being significantly lower when dispersed in stain. In this matrix, cerium release through simulated dermal contact is lower than 2.5 mg/m^2. Alternatively, the release from water-based applications is initially as high as 21 mg/m^2 and decays to a steady state of approximately 4 mg/m^2 after 4 weeks of UV exposure and sampling.

To understand the effect of surface degradation on the cerium release, a direct comparison of release from the UV-aged boards and a control system is necessary. However, the boards degraded in the UV light chamber were sampled over an 8-week period, while control boards were sampled over an interval of 6 months. To compare these data sets, the cerium release is plotted in terms of the corresponding wipe event, regardless of the time, and presented in Figure 5. Clearly, there is no difference in release from these two treatments when the ceria NPs are dispersed in water. When dispersed in stain, a significant difference in release is found at the initial sampling event. This difference might be a result of moisture loss from the aged boards during the 1260 h of UV exposure. Consequently, the stain formulation is more effectively drawn into wood pores during application, resulting in a lower cerium release during the initial wipe event. This analysis appears to indicate that the total number of contact events drive long-term cerium release, regardless of the weathering condition. However, the age of the coated surface, as well as the dispersion medium (*i.e.*, water vs. stain) will play a role in the initial release characteristics.

Characterization of Cerium Released Through Simulated Dermal Contact:

Results from wiping studies indicate that a significant portion of cerium may be released through dermal contact, especially during early contact events. However, a detailed understanding of the form and speciation of cerium released from the surface is critical in assessing human and environmental health risks. As described in the Methods section, a single cloth from the dermal transfer experiments was extracted with water and sequential filtered. In all cases, large differences in cerium concentration were observed between unfiltered samples and 0.45μm filtrate, indicating retention of cerium particulate matter on the filters. Therefore, these filters were reserved and analyzed for particle morphology using a FESEM with EDS capabilities. A representative Backscattered Electron (BSE) FESEM image of particulate matter captured on these filters from Water/Wood treatments is shown in Figure 6. A variety of particle sizes and morphologies are retained on the 0.45 μm filter during extraction. The vast majority appear to be large wood aggregates ranging between roughly 1 to 10 μm. These larger aggregates are similar to the size and shape of material dislodged from uncoated MCA boards during identical wiping tests by Platten and coworkers when investigating potential Cu NP release from these products (Platten III et al., 2016). Indeed, the EDS micrographs show a heavy collocation of cerium with copper, indicating that the cerium remains attached to the wood aggregates that are removed from the surface during simulated dermal contact. From the collected images, it does not appear

that significant portions of free ceria nanoparticles are released from the surface during wiping events.

BSE-FESEM images of Stain/Wood samples show a similar size distribution of particulate matter retained on the filters (Figure S8). Interestingly, abundant amounts of silica, aluminum, and iron particles are found instead of copper. This can be attributed to the complex nature of the stain, which includes significant concentrations of these elements in its formulation. Similar analysis of the filters from Water/Composite treatments again show the larger aggregates containing cerium retained on the filter. The larger fragments may be from the plastic capping agent used on the composite decking surface that was removed/ dislodged from the surface during sampling (Figure S9).

While BSE-FESEM images indicate the release of larger aggregates during simulated dermal contact, the speciation of cerium in these samples is also critical to evaluate potential ecological and human health risks. The results of the XAFS speciation analysis are presented in Table 2. As major differences in the LCF fits between normalized and first derivative of normalize spectra were not significant, results from first derivative spectra were adopted and presented here. It is generally accepted that the inherent error in any LCF analysis is between 5 percent to 10 percent (Gräfe et al., 2014). Examples of reference spectra and LCF fits are presented in the Supporting Information (Figures S10 and S11). It is clear from the LCF analysis that the vast majority of material extracted from the cloths used in the CPSC test method remain CeO_2 (> 70%) throughout weathering and release. This result agrees with Auffan and coworkers who also reported on the high stability of CeO_2 NPs over 112 days of UV degradation (Auffan et al., 2014). After extended weathering (~16 weeks), there is a conversion of the parent material to a Ce(III)-organic species modeled as Ce(III)-Oxalate. In fact, CeO_2 dispersion and application in the wood stain may stimulate an initial release of Ce(III) during the solution preparation stage as the organics present in the stain complex with the cerium particle surface. However, the continued reduction of Ce(IV) to Ce(III) is limited when compared to the same transformation in water-based formulations over the same sampling period. Interestingly, when applied to the composite material, the initial CeO_2 particles remain stable for the first 3 months of exposure. It is possible that the cerium reduction seen in dispersions applied to wood surfaces may involve a redox cycling between the Ce particles added as coatings and the copper particles abundantly distributed though the MCA treated lumber (Evans et al., 2012; Matsunaga et al., 2009). The release of Ce(III) species during the weathering process is in contrast with the underlying selection of CeO_2 as a UV-protective additive to surface coatings. A driver for the selection of CeO_2 has been its perceived crystallinity and stability (Batley et al., 2013; Cornelis et al., 2011; Dahle et al., 2015). The results presented here suggest the potential for the slow conversion and release of CeO_2 to Ce(III) species over long weathering periods.

To ensure that the transformation of Ce(IV) to Ce(III) in the filter samples was not a result of the wipe extraction and sequential filtration, subsamples of both outdoor weathered and indoor control samples were scraped from the surface after the 6-month sampling period. The resulting sawdust was pressed into 13 mm diameter pellets and analyzed for cerium speciation using XAFS with no further processing. The result of the LCF analysis for these samples is also shown in Table 2. Cerium speciation in the sawdust pellets confirms the

presence of Ce(III) on the wood surfaces after 6 months of weathering, particularly for the outdoor samples. As the indoor samples were kept covered at a constant temperature with no UV exposure, the persistence of CeO_2 is expected. It is clear that CeO_2 particles dispersed in water are more readily converted to a Ce(III) species as compared to the same particles dispersed in a more complex stain matrix. Roughly 30 percent of the initially applied CeO_2 has been reduced to Ce(III) when applied in Milli-Q water, while stain-based applications only show 7 percent of the applied cerium undergoing the same reduction. Additional research is needed to determine the extent and conditions that drive this release and potential human and environmental risk.

Cerium Release from Simulated Leaching:

Total cerium concentrations found in all three fractions collected from the simulated leaching procedure are outlined in Figure 7. In general, the concentrations of cerium release after a 72-h period are low, with the highest concentration determined to be 0.662 mg/L. Similar to the results from studies on simulated dermal transfer, the dispersion solution (*i.e.*, water or stain) has a significant effect on the cerium release. MCA samples coated with CeO_2 dispersed in wood stain resulted in cerium concentrations below the method detection limit (MDL) for all replicates. This same trend is evident for composite samples treated with CeO_2 dispersed in water. Although each of these experimental treatments resulted in cerium concentrations below the MDL, it does not imply that there is no cerium leached from the surface. We attribute this lack of detectable cerium release from stain/wood samples to be a function of the polymers and binders in the stain matrix, sealing the NPs in the wood. The lack of release from the water/composite samples is more difficult to explain. During the simulated dermal transfer experiments previously discussed, cerium was readily removed from the surface, which was not reproduced during leaching. The differences between the wiping and leaching tests may also be explained by the nature of the experiments. Wiping experiments physically abrade the surface during testing, promoting surface release, while the leaching study may be considered a more passive release test.

In the case of water/wood treatments, the vast majority (~80%) of the cerium found in the unfiltered leachate passed through each of the subsequent filters (0.45 μm and 10 kDa). This behavior indicates low levels of ionic cerium released from the wood surface during leaching. LCF analysis of XAFS spectra obtained on the wood blocks before and after leaching is shown in Table 3. Similar to the wiping experiments, both the initial CeO_2 material and a Ce(III)-Oxalate standard were used to model cerium speciation. In all cases, CeO_2 is the major component both before and after leaching in SPLP solution. After leaching, minor changes to the relative percentages of the two-component system are evident. However these changes are not significant when you consider the inherent 5 percent to 10 percent error in LCF analysis (Gräfe et al., 2014).

While the bulk cerium speciation on the coated surfaces remains constant both before and after leaching in SPLP solution, there is evidence of potential release of Ce(III) during leaching tests. XAFS spectra of filters produced during leaching of water/composite samples shows clear evidence of Ce(III) in normalized spectra seen in Figure 8. Although ICP analysis was unable to detect cerium above the MDL in each of the filtrate fractions, any

cerium retained on the filters is highly concentrated compared to the diffuse cerium released into the leachate allowing for fluoresce data collection under optimal conditions. XAFS analysis of the 10 kDa filter shows clear features of both the Ce(III) and Ce(IV) oxidation states. Collectively, the results of the leaching studies on all of the experimental treatments indicate that while the vast majority of the initial material remains as the applied CeO_2 NPs, there is potential for the release of ionic cerium in both the (III) and (IV) oxidation state. Additional research is needed to determine factors that drive the transformation and release of these materials during the use phase, especially focusing on the medium in which the NPs will be dispersed and applied.

Cerium Exposure Assessment:

The potential toxicity of CeO_2 particles has been controversial in the peer-review literature. Their redox activity has been cited as the cause of both its antioxidant capabilities, as well as its potential to generate harmful reactive oxygen species (ROS) during exposure (Dahle and Arai, 2015; Li et al., 2016). Although the current state of knowledge on CeO_2 NP toxicity remains limited, the results of the wipe experiments are useful in determining realistic exposure concentrations from dermal contact during intended-use scenarios. Using the manufacturer's recommendations, significant amounts of CeO_2 were applied to both MCA lumber and composite decking. The coatings procedure resulted in approximately 110 mg of CeO_2 on each 2 ft test section of the MCA lumber and composite decking, respectively. This concentrated application of CeO_2 represents a targeted area of potential human and environmental exposure.

It is clear that cerium release is highest during the initial dermal contact events (Figures 2–5, S6–S7). The largest mass of cerium (Ce) release from a single wipe event (10 wipes of a 450 cm^2 area) was approximately 1 mg Ce, while the total mass of Ce collected over the course of the 6-month weathering period for an individual treatment did not exceed 3 mg. (Figures S7–S8) Importantly, CeO_2 NPs dispersed in wood stain are more resistant to release compared to the same particles dispersed in Milli-Q water. There have been few published studies on the biological effects of ingested CeO_2 NPs. However, a recent study by Kumari and coworkers on the acute oral toxicity of CeO_2 NPs to Wistar rats found no significant toxicity at or below 500 mg Ce/kg body weight (Kumari et al., 2014). The total amount of cerium collected from dermal transfer wipes is at least two orders of magnitude below this potential toxicity threshold, even if it is assumed that a single individual ingested the entire mass of cerium release during the 6-month experimental duration. Critically, the study by Kumari and coworkers did not investigate the effect of cerium speciation on the potential toxicity (Kumari et al., 2014). XAFS analysis of both the particulate material retained on 0.45μm filters and board surfaces indicated as much as 30 percent of the initial CeO_2 had been converted to a Ce(III)-organic species. Previous work has demonstrated differences in biological response based on cerium oxidation state. For example, Dahle and Arai found that soluble Ce(III) was more toxic to microbes governing soil denitrification than CeO_2 particles at subchronic toxicity doses (Dahle and Arai, 2014). Several recent articles have evaluated the health effects of repeated oral exposure to CeO_2 (Hirst et al., 2013; Kumari et al., 2014; Yokel et al., 2014). Adverse health effects were only noted at cerium concentrations exceeding 100 mg/kg bodyweight, roughly 30 times greater than the highest amount of

cerium wiped from the aqueous application to composite material over the entire sampling period. As previously discussed, the amount of CeO_2 applied to the wood surface for the aqueous and stain applications was ~1180 mg/m^2 or 0.12 mg/cm^2, respectively. Even if whole pieces of wood broken away from the surface were ingested, the dose would be well below the reported concentrations associated with adverse health effects.

Regarding cerium release during leaching experiments, the highest concentration found in any of the leached samples was 0.662 mg/L. This leached concentration is significantly lower than previously reported EC50 values in a simple aquatic test organism (*Pseudokirchneriella subcapitata*); values ranging from approximately 2–30 mg/L, depending on particle size and test conditions (Hoecke et al., 2009; Rodea-Palomares et al., 2011; Rogers et al., 2010). Similar to the wipe results, ecological risk is mitigated when the ceria NPs are dispersed in a wood stain for application (Figure 7).

A secondary result of this comprehensive release analysis using both dermal contract and leaching studies indicates how the type of test may drastically affect the perceived risk of an ENM-enabled product. For example, the results of the wipe analysis on composite decking samples coated with water dispersed CeO_2 show a high likelihood of release, especially during the initial contact events (~18 mg/m^2 Ce). However, leaching studies using identical samples resulted in cerium concentrations below the MDL. While the differences in the results can be explained by the nature of the experiments (physical abrasion vs. passive release), relying on a single test results in an inaccurate description of the potential risks. The results of both wiping and leaching experiments demonstrate the necessity of evaluating ENM release during simulated use scenarios. To accurately assess the potential toxicity of ENM in consumer products, detailed information on both the total concentration and form of material release is critical for proper risk analysis.

Implications and Future Research Directions

Understanding the release of nanomaterials from consumer products during the use phase is a critical component in determining their environmental and human health risk. Special attention must be paid to ENM containing or ENM enabled surface coatings as they are readily available for transformation and release, potentially more so than products with embedded ENMs. The results of this study highlight the important role that dispersion media plays in both release and chemical transformation of NPs. In both leaching and wiping studies, cerium release was higher when dispersed in Milli-Q water than wood stain. Furthermore, chemical conversion of the pristine CeO_2 to a Ce(III) organic species was readily apparent in the water-dispersed treatments. Even with these changes in chemical speciation, the results suggest that while weathering conditions may serve to affect the cerium release during simulated dermal contact, the most critical factor affecting the extent of release is the number of contact events (Figure 5).

While there has been significant investment in understanding the toxicity of pristine engineered nanoparticles, more research must be conducted on understanding their transformation and release during realistic use scenarios. In some cases, these transformed particles and byproducts may have more divergent environmental and human health impacts

than their pristine parent material. Future research should focus on establishing standard methods to track NP degradation and release from nano-enabled products during their life-cycle to properly assess both the near-field and long-range implications. The data presented here demonstrate the potential utility of the CPSC wipe methodology as a simple screening assay for NP release and exposure by dermal contact. Information gathered from these simple, reproducible techniques is incredibly valuable to properly evaluate the true environmental and human health risks associated with nano-enabled consumer products.

Supplementary Material

Refer to Web version on PubMed Central for supplementary material.

Acknowledgements

Any opinions expressed in this paper are those of the authors(s) and do not, necessarily, reflect the official positions and policies of the U.S. EPA or the U.S. CPSC. Any mention of products or trade names does not constitute recommendation for use by the U.S. EPA or U.S. CPSC. Thanks to Jennifer Goetz for engineering support with the UV light chamber. Use of the Advanced Photon Source (APS), a U.S Department of Energy (DOE) Office of Science User Facility operated for the DOE Office of Science by Argonne National Laboratory under Contract No. DE-AC0206CH1357. MRCAT operations (Sector 10) are supported by the DOE and the MRCAT member institutions. This project was supported, in part, by an appointment in the Research Participation Program at the Office of the Research and Development (ORD), EPA administered by the Oak Ridge Institute for Science and Education through an interagency agreement between the DOE and EPA.

References

Al-Kattan A, Wichser A, Vonbank R, Brunner S, Ulrich A, Zuin S, et al. Characterization of materials released into water from paint containing nano-SiO2. Chemosphere 2015; 119: 1314–1321. [PubMed: 24630447]

Al-Kattan A, Wichser A, Vonbank R, Brunner S, Ulrich A, Zuin S, et al. Release of TiO_2 from paints containing pigment-TiO_2 or nano-TiO_2 by weathering. Environmental Science: Processes & Impacts 2013; 15: 2186–2193. [PubMed: 24056809]

Auffan M, Masion A, Labille J, Diot M-A, Liu W, Olivi L, et al. Long-term aging of a CeO_2 based nanocomposite used for wood protection. Environmental Pollution 2014; 188: 1–7. [PubMed: 24518963]

Batley GE, Halliburton B, Kirby JK, Doolette CL, Navarro D, McLaughlin MJ, et al. Characterization and ecological risk assessment of nanoparticulate CeO2 as a diesel fuel catalyst. Environmental Toxicology and Chemistry 2013; 32: 1896–1905. [PubMed: 23595783]

Castano CE, O'Keefe MJ, Fahrenholtz WG. Cerium-based oxide coatings. Current Opinion in Solid State and Materials Science 2015; 19: 69–76.

Cobb D Cromated Copper Arsenic (CCA) CCA-treated Wood Analysis Memorandum from David Cobb to Patricia Bittner. U.S. Consumer Product Safety Commission, Washington, DC, 2003.

Collin B, Auffan M, Johnson AC, Kaur I, Keller AA, Lazareva A, et al. Environmental release, fate and ecotoxicological effects of manufactured ceria nanomaterials. Environmental Science: Nano 2014; 1: 533–548.

Cornelis G, Ryan B, McLaughlin MJ, Kirby JK, Beak D, Chittleborough D. Solubility and Batch Retention of CeO2 Nanoparticles in Soils. Environmental Science & Technology 2011; 45: 2777–2782. [PubMed: 21405081]

Dahle J, Arai Y. Environmental Geochemistry of Cerium: Applications and Toxicology of Cerium Oxide Nanoparticles. International Journal of Environmental Research and Public Health 2015; 12: 1253. [PubMed: 25625406]

Dahle JT, Arai Y. Effects of Ce(III) and CeO2 Nanoparticles on Soil-Denitrification Kinetics. Archives of Environmental Contamination and Toxicology 2014; 67: 474–482. [PubMed: 24760446]

Dahle JT, Livi K, Arai Y. Effects of pH and phosphate on CeO2 nanoparticle dissolution. Chemosphere 2015; 119: 1365–1371. [PubMed: 24630459]

Deshpande S, Patil S, Kuchibhatla SV, Seal S. Size dependency variation in lattice parameter and valency states in nanocrystalline cerium oxide. Applied Physics Letters 2005; 87: 133113.

Evans PD, Limaye A, Averdunk H, Turner M, Senden T, Knackstedt M. Use of X-Ray Micro-Computed Tomography to Visualize Copper in Preservative Treated Wood. International Research Group On Wood Protection 43rd Annual Meeting Proceedings, 2012.

Faure B, Salazar-Alvarez G, Ahniyaz A, Villaluenga I, Berriozabal G, Miguel YRD, et al. Dispersion and surface functionalization of oxide nanoparticles for transparent photocatalytic and. Science and Technology of Advanced Materials 2013; 14: 023001. [PubMed: 27877568]

Gräfe M, Donner E, Collins RN, Lombi E. Speciation of metal(loid)s in environmental samples by X-ray absorption spectroscopy: A critical review. Analytica Chimica Acta 2014; 822: 1–22. [PubMed: 24725743]

Hirst SM, Karakoti A, Singh S, Self W, Tyler R, Seal S, et al. Bio-distribution and in vivo antioxidant effects of cerium oxide nanoparticles in mice. Environmental Toxicology 2013; 28: 107–118. [PubMed: 21618676]

Hochella MF. Auger Electron and X-Xay Photoelectron Spectroscopies In: Hawthorne FC, editor. Reviews in Minerology: Spectroscopic Methods in Minerlogy and Geology. 18 Mineralogical Society of America, Washington D.C., 1988.

Hoecke KV, Quik JTK, Mankiewicz-Boczek J, Schamphelaere KACD, Elsaesser A, Meeren PVd, et al. Fate and Effects of CeO2 Nanoparticles in Aquatic Ecotoxicity Tests. Environmental Science & Technology 2009; 43: 4537–4546. [PubMed: 19603674]

Hwang DK, Moon JH, Shul YG, Jung KT, Kim DH, Lee DW. Scratch Resistant and Transparent UV-Protective Coating on Polycarbonate. Journal of Sol-Gel Science and Technology 2003; 26: 783–787.

Kaegi R, Sinnet B, Zuleeg S, Hagendorfer H, Mueller E, Vonbank R, et al. Release of silver nanoparticles from outdoor facades. Environmental Pollution 2010; 158: 2900–2905. [PubMed: 20621404]

Kaegi R, Ulrich A, Sinnet B, Vonbank R, Wichser A, Zuleeg S, et al. Synthetic TiO2 nanoparticle emission from exterior facades into the aquatic environment. Environmental Pollution 2008; 156: 233–239. [PubMed: 18824285]

Kaiser J-P, Roesslein M, Diener L, Wick P. Human health risk of ingested nanoparticles that are added as multifunctional agents to paints: an in vitro study. PloS one 2013a; 8: e83215. [PubMed: 24358264]

Kaiser J-P, Zuin S, Wick P. Is nanotechnology revolutionizing the paint and lacquer industry? A critical opinion. Science of The Total Environment 2013b; 442: 282–289. [PubMed: 23178832]

Keller AA, McFerran S, Lazareva A, Suh S. Global life cycle releases of engineered nanomaterials. Journal of Nanoparticle Research 2013; 15: 1–17.

Kropf AJ, Katsoudas J, Chattopadhyay S, Shibata T, Lang EA, Zyryanov VN, et al. The New MRCAT (Sector 10) Bending Magnet Beamline at the Advanced Photon Source. AIP Conference Proceedings 2010; 1234: 299–302.

Kumari M, Kumari SI, Kamal SSK, Grover P. Genotoxicity assessment of cerium oxide nanoparticles in female Wistar rats after acute oral exposure. Mutation Research/Genetic Toxicology and Environmental Mutagenesis 2014; 775–776: 7–19.

Lee J, Mahendra S, Alvarez PJJ. Nanomaterials in the Construction Industry: A Review of Their Applications and Environmental Health and Safety Considerations. ACS Nano 2010; 4: 3580–3590. [PubMed: 20695513]

Lee SS, Song W, Cho M, Puppala HL, Nguyen P, Zhu H, et al. Antioxidant Properties of Cerium Oxide Nanocrystals as a Function of Nanocrystal Diameter and Surface Coating. ACS Nano 2013; 7: 9693–9703. [PubMed: 24079896]

Li Y, Li P, Yu H, Bian Y. Recent advances (2010–2015) in studies of cerium oxide nanoparticles' health effects. Environmental Toxicology and Pharmacology 2016; 44: 25–29. [PubMed: 27088851]

Manoudis PN, Tsakalof A, Karapanagiotis I, Zuburtikudis I, Panayiotou C. Fabrication of super-hydrophobic surfaces for enhanced stone protection. Surface and Coatings Technology 2009; 203: 1322–1328.

Matsunaga H, Kiguchi M, Evans PD. Microdistribution of copper-carbonate and iron oxide nanoparticles in treated wood. Journal of Nanoparticle Research 2009; 11: 1087–1098.

Piccinno F, Gottschalk F, Seeger S, Nowack B. Industrial production quantities and uses of ten engineered nanomaterials in Europe and the world. Journal of Nanoparticle Research 2012; 14: 1–11. [PubMed: 22448125]

Platten III WE, Sylvest N, Warren C, Arambewela M, Harmon S, Bradham K, et al. Estimating dermal transfer of copper particles from the surfaces of pressure-treated lumber and implications for exposure. Science of The Total Environment 2016; 548–549: 441–449. [PubMed: 27371770]

Ravel B, Newville M. ATHENA, ARTEMIS, HEPHAESTUS: data analysis for X-ray absorption spectroscopy using IFEFFIT. J. Synchrotron Radiat. 2005; 12: 537–541. [PubMed: 15968136]

Rodea-Palomares I, Boltes K, Fernández-Piñas F, Leganés F, García-Calvo E, Santiago J, et al. Physicochemical Characterization and Ecotoxicological Assessment of CeO2 Nanoparticles Using Two Aquatic Microorganisms. Toxicological Sciences 2011; 119: 135–145. [PubMed: 20929986]

Rogers NJ, Franklin NM, Apte SC, Batley GE, Angel BM, Lead JR, et al. Physico-chemical behaviour and algal toxicity of nanoparticulate CeO2 in freshwater. Environmental Chemistry 2010; 7: 50–60.

Sawitowski RHCaT. The Impact of Nano-Materials on UV-Protective Coatings. NSTI Nanotechnology Conference and TRade Show. 1, 2006, pp. 230–230.

Shandilya N, Le Bihan O, Bressot C, Morgeneyer M. Emission of Titanium Dioxide Nanoparticles from Building Materials to the Environment by Wear and Weather. Environmental Science & Technology 2015; 49: 2163–2170.

Thomas TA, Levenson MS, Cobb DG, Midgett JD, Porter WK, Saltzman LE, et al. The Development of a Standard Hand Method and Correlated Surrogate Method for Sampling CCA (Pressure)-Treated Wood Surfaces for Chemical Residue. Journal of Children's Health 2005; 2: 181–196.

van Broekhuizen P, van Broekhuizen F, Cornelissen R, Reijnders L. Use of nanomaterials in the European construction industry and some occupational health aspects thereof. Journal of Nanoparticle Research 2011; 13: 447–462.

Yokel RA, Hussain S, Garantziotis S, Demokritou P, Castranova V, Cassee FR. The yin: an adverse health perspective of nanoceria: uptake, distribution, accumulation, and mechanisms of its toxicity. Environmental Science-Nano 2014; 1: 406–428. [PubMed: 25243070]

Zhang H, He X, Zhang Z, Zhang P, Li Y, Ma Y, et al. Nano-CeO2 Exhibits Adverse Effects at Environmental Relevant Concentrations. Environmental Science & Technology 2011; 45: 3725–3730. [PubMed: 21428445]

Zhou S, Wu L, Sun J, Shen W. The change of the properties of acrylic-based polyurethane via addition of nano-silica. Progress in Organic Coatings 2002; 45: 33–42.

Zuin S, Gaiani M, Ferrari A, Golanski L. Leaching of nanoparticles from experimental water-borne paints under laboratory test conditions. Journal of Nanoparticle Research 2013; 16: 1–17.

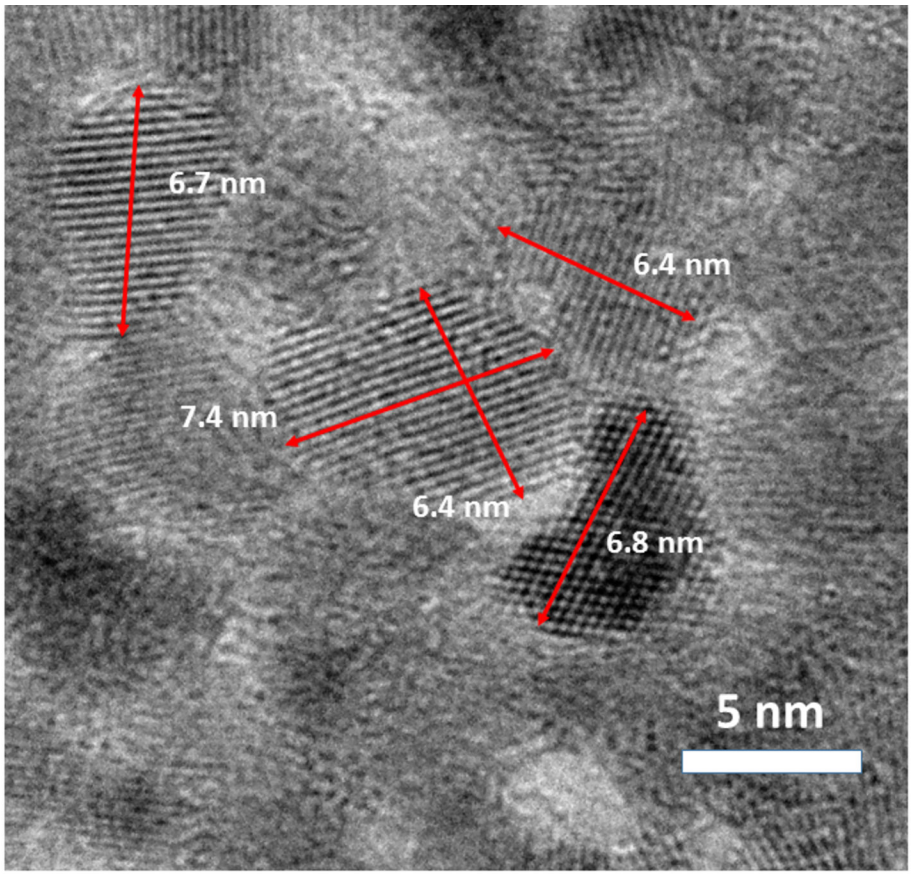

Figure 1:
STEM images of CeO_2 NPs used in this study. Particle size was calculated as 6.4±1.3 nm by manual analysis of 53 particles.

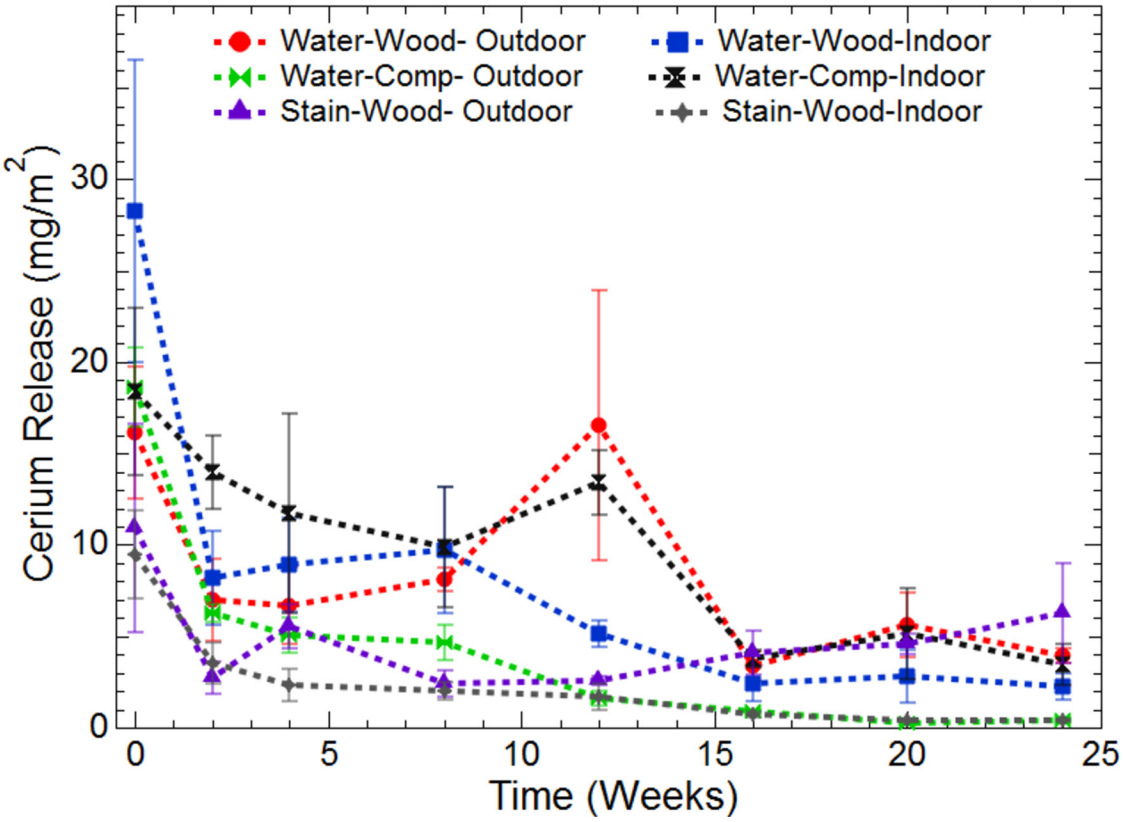

Figure 2:

Release of cerium from coated boards. Data for both weathered boards (Outdoor) and controls (Indoor) are an average of at least three separate replicates. Time zero corresponds with the first wipe event after application of surface coatings and dry time of at least 48 h. Data has been normalized based on the area wiped per sampling event.

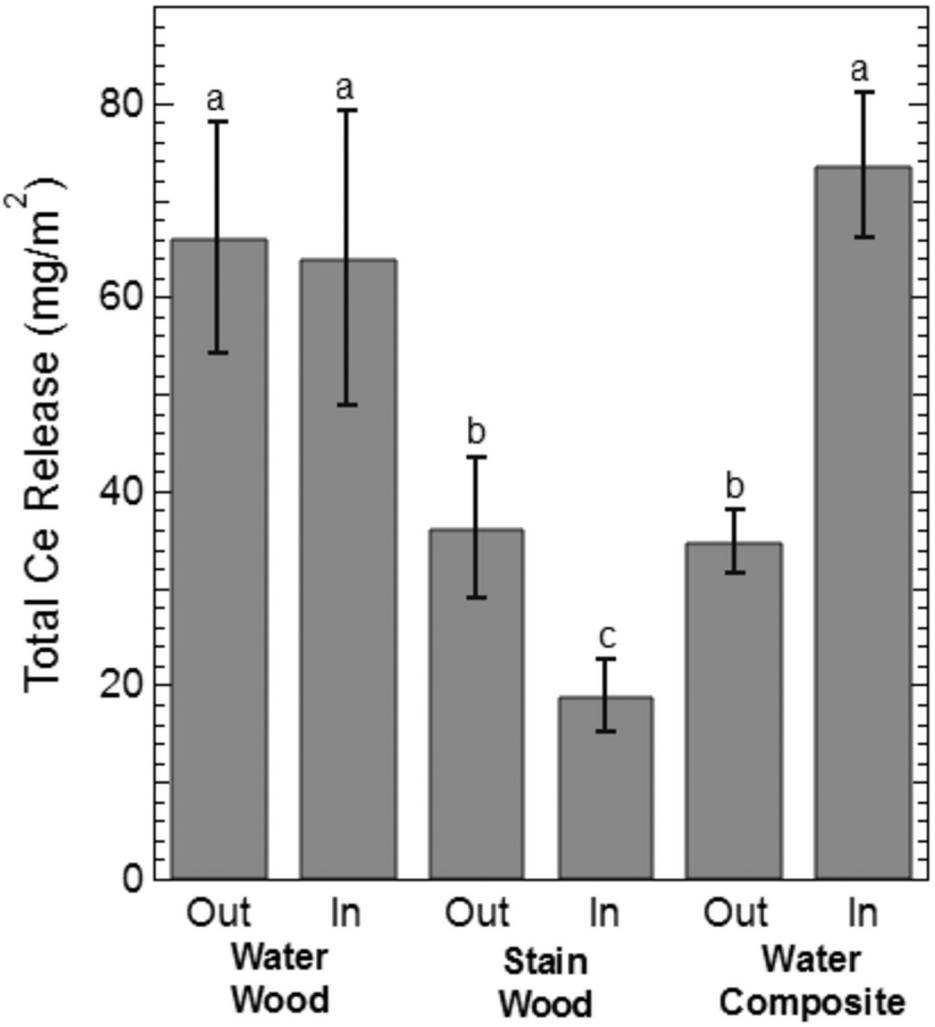

Figure 3:

Total cerium wiped from the surface of the wood and composite surfaces for the outdoor and indoor treatments. The Out and In designations refer to whether the surfaces coating were aged outdoors (Out) or indoors (In). Indoor samples function as experimental controls for outdoor samples. The lower-case letters indicate statistical differences in the mean concentration of cerium wiped from the surface over the 6-month experiment as determined by a Fisher LSD means test (n= 4; $\alpha = 0.05$). Identical letters indicate no statistical difference in the mean.

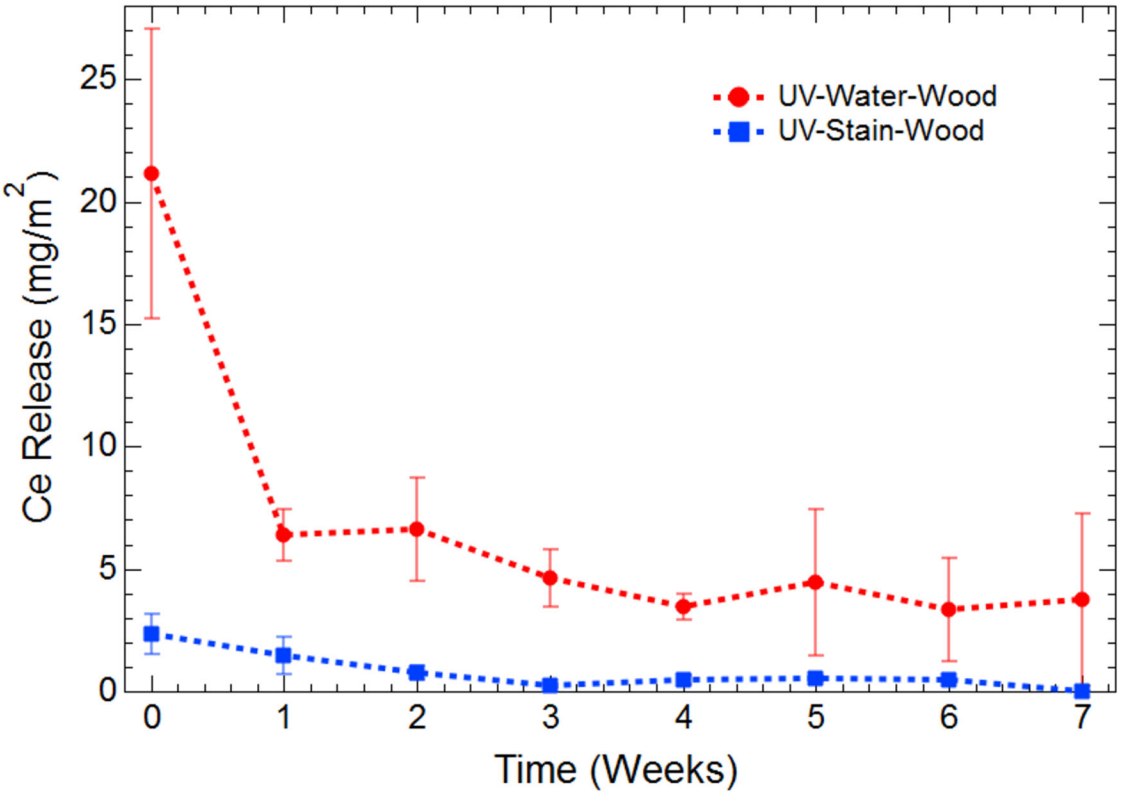

Figure 4:

Release of cerium from MCA-coated boards that have undergone 1260 h of UV degradation before application of surface coatings. Data were collected in triplicate and have been normalized by the total area wiped during a sampling event. The data at Time zero correspond with the first wipe event after application of surface coatings and dry time of at least 48 h.

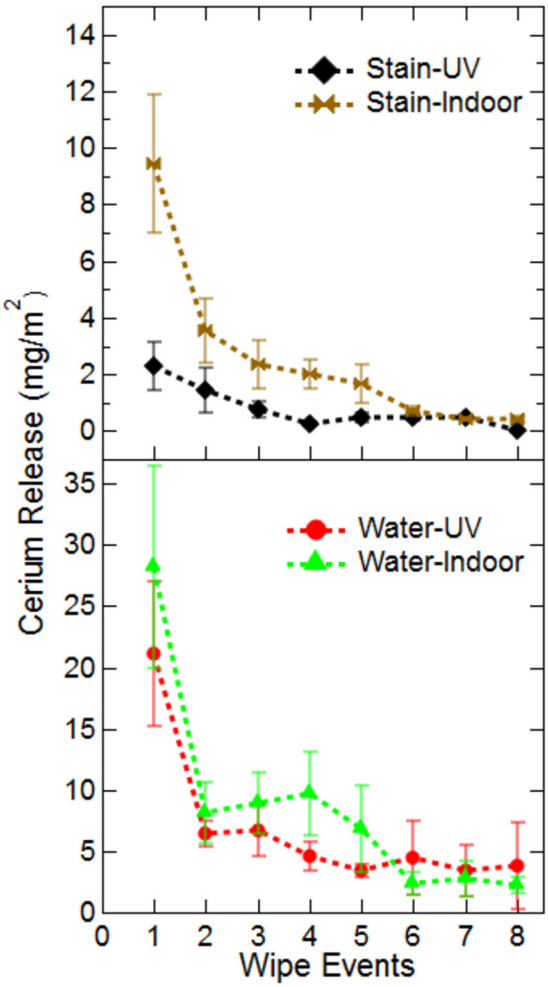

Figure 5:

Release of cerium from pristine MCA boards (controls) and UV degraded boards per wipe event. Data were collected in triplicate and have been normalized by the total area wiped during a sampling event.

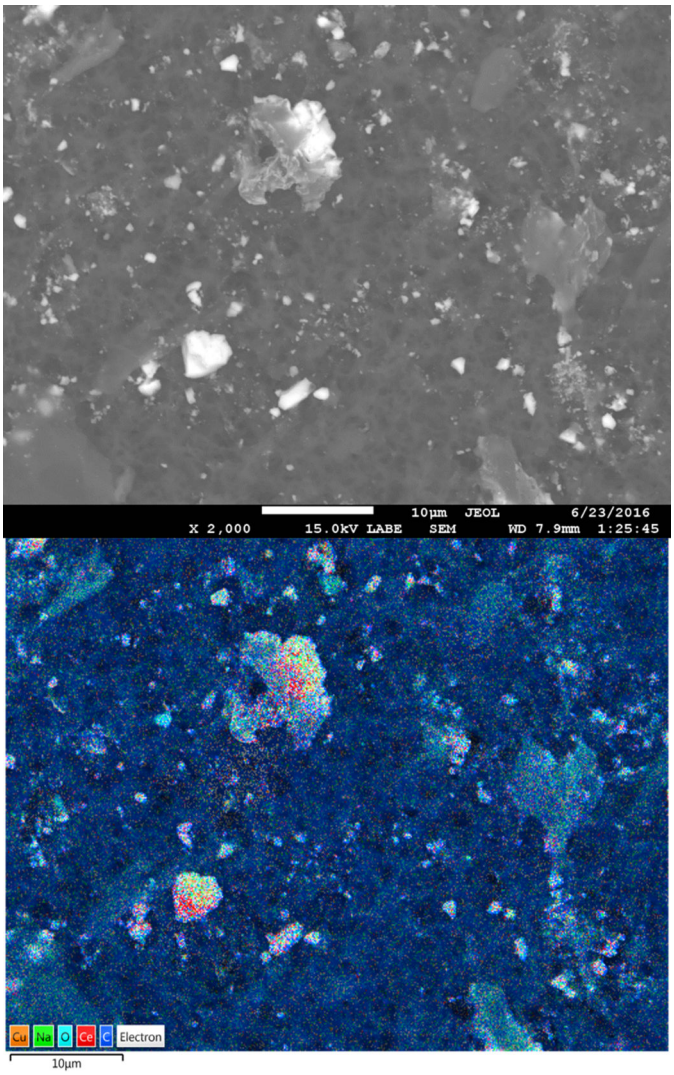

Figure 6:

SEM image of particulate matter retained on a 0.45µm filter after release and extraction using the CPSC estimate of dermal transfer test method. Sample is from a micronized copper pressure-treated lumber coated with CeO_2 NPs dispersed in water after 1 month of outdoor weathering. Cerium particles are heavily co-located with copper particles, as shown in the EDS micrograph.

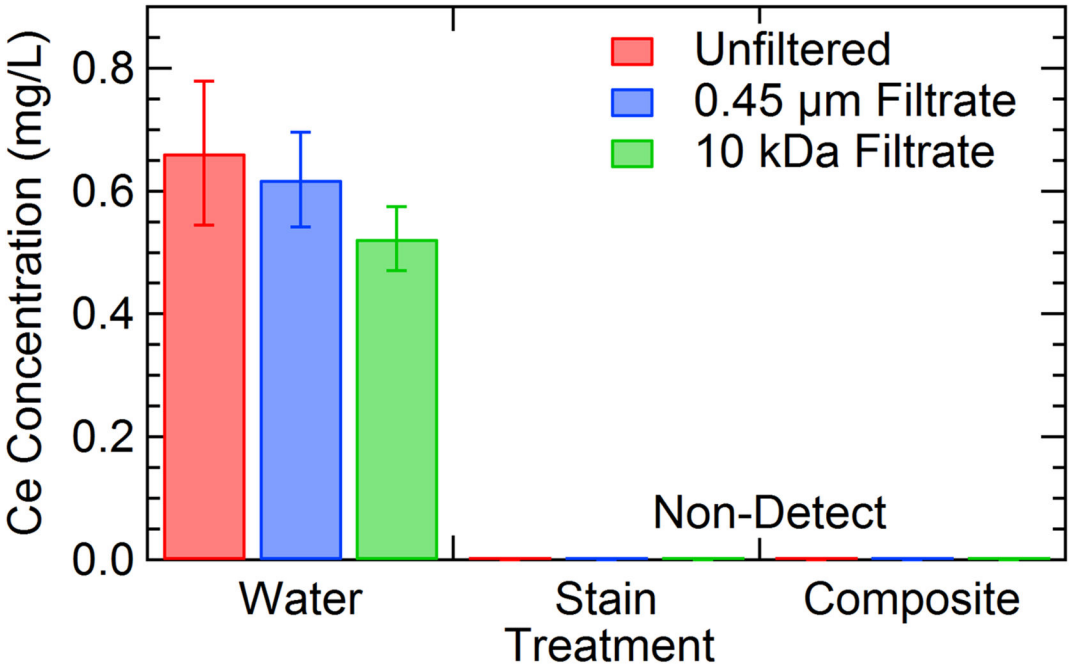

Figure 7:

Results of leaching test performed on surface coupons that had been painted with different experimental treatments. Samples were allowed to mix in SPLP solution for 72 h and then sequential filtered to determine size fractions of released material. Composite samples are coated with CeO2 dispersed in water as wood stain is not intended for application on composite surfaces. Detection limit for this analysis is 0.230 mg/L Ce.

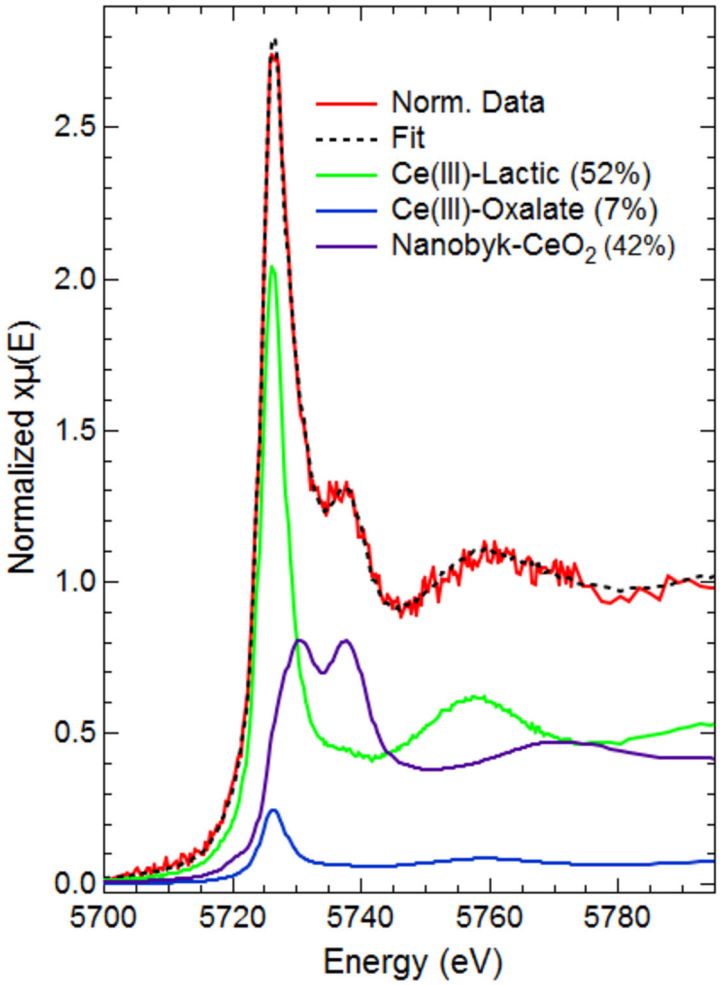

Figure 8:

XAFS data collected on a 10 kDa filter produced after leaching a CeO2/Water/Composite sample in SPLP solution for 72 h. Resulting data clearly demonstrate the presence of both Ce(III) and Ce(IV) oxidation states.

Table 1:

Summary of initial characterization of CeO_2 NPs used throughout this study. Particle size estimates derived from STEM images are produced through measurement of 53 particles. Large discrepancy in the Ce speciation between XPS and XAFS techniques is based on differences in surface sensitivity.

Particle Size	
Technique	
Manufacturer Listed	10 nm
Hydrodynamic Diameter (HDD)	8.16 nm +/− 0.09
STEM	6.4 nm +/− 1.3

Cerium Speciation		
Technique	***Ce(III)***	***Ce(IV)***
XPS	56–64%	44–36%
XAFS	-	100%

Table 2:

Summary of cerium speciation extracted from CPSC wipe method cloths determined by LCF analysis of first derivate of normalized XAFS Spectra. Samples marked N/A have cerium concentration low enough creating insufficient signal-to-noise ratios during XAFS data collection and were not used in LCF analysis.

Cerium - Water- Composite								
Species	Time Zero	2 Weeks	4 Weeks	8 Weeks	12 Weeks	16 Weeks	20 Weeks	24 Weeks
CeO_2	100	100	100	100	N/A	70	N/A	N/A
Ce(III) Oxalate	0	0	0	0	N/A	30	N/A	N/A
Cerium - Water- Wood								
CeO_2	100	100	95	91	92	79	73	N/A
Ce(III) Oxalate	0	0	5	9	8	21	27	N/A
Cerium - Stain - Wood								
CeO_2	100	95	91	86	94	88	N/A	N/A
Ce(III) Oxalate	0	5	9	14	6	12	N/A	N/A
Sawdust Surfaces								
Species	Water/Wood/Indoor		Water/Wood/Outdoor		Stain/Wood/Indoor		Stain/Wood/Outdoor	
CeO_2	98		70		100		93	
Ce(III) Oxalate	3		30		0		7	

Table 3:

Summary of cerium speciation on wood blocks coated with CeO_2 NP dispersed in either Milli-Q water or wood stain before and after 72 hours of leaching in 100 mL of SPLP solution. LCF results were derived from analysis of first derivative of normalized spectra using three cerium standards.

Water/Wood	**Water/Wood**		**Stain/Wood**		**Water/Composite**	
Species	*Pristine*	*Leached*	*Pristine*	*Leached*	*Pristine*	*Leached*
CeO_2	96	92	93	91	94	98
Ce(III)-Oxalate	4	7	7	9	6	2